

HIGH RATE DELAMINATION FRACTURE OF AEROSPACE COMPOSITES

Anastasios Toulitsis¹, Stefanos Giannis¹

¹Element Materials Technology, Wilbury Way, Hitchin SG4 0TW, UK
Email: anastasios.toulitsis@element.com, stefanos.giannis@element.com,
Web Page: www.element.com

Keywords: Delamination, Mode I, Mode II, High Rate, Software

Abstract

In this research work, the effect of test rate on the fracture toughness under Mode I and Mode II loading conditions for a carbon fibre reinforced composite material was investigated. A range of test speeds up to 1 m/s were studied. Software was developed to capture the delamination growth at higher test rates, using the recorded video from the test. For Mode I tests, the conventional double cantilever beam (DCB) configuration was used for lower test rates, but a wedge test setup was used for elevated speeds to reduce the inertia effects and ensure the symmetrical load application on the specimen. For the Mode II tests, the End-Loaded Split (ELS) configuration was used at all test rates. For both loading modes the Critical Strain Energy Release Rates (G_{Ic} and G_{IIc}) were found to be unaffected by the different test rates. In specimens tested in Mode I it was found that delamination propagated in a stable manner for all test rates. The G_{IIc} was evaluated for the point of deviation from linearity and the point of maximum load, since the delamination propagation was unstable for all test rates in Mode II.

1. Introduction

Developing damage tolerance design methodologies and accounting for delamination initiation and growth in composite structures requires the characterisation of the material's delamination. Fracture tests on unidirectional reinforced specimens are used to characterise delamination initiation and growth under quasi-static and fatigue loading. Nowadays, there are standard procedures for measuring the strain energy release rates of unidirectional laminates (UD). They include both Mode I and Mode II test configurations.

The widely spread test method for measuring the G_{Ic} is according to ASTM D5528 [1], where the opening load is transferred to the DCB specimen by using piano hinges or loading blocks. The initial delamination in the specimen is created by a non-stick (PTFE) insert. More recently a standard procedure for measuring the G_{IIc} using the ELS test method has been published. The ISO 15114 [2] presents the standard procedure parameters for measuring the G_{IIc} . Similar specimens as in Mode I tests are used. However, the loading condition differs from Mode I, since now the specimen is clamped at one side, whereas the load is applied in the side which contains the initial delamination and the loading block. Loading in bending induces shear stresses on the delamination surfaces.

Nevertheless, most of the composite structures face dynamic loading conditions, which differs from the established quasi-static testing. Composites are viscoelastic materials, so the response in quasi-static and dynamic loading may be differ. As a result, the interest of the failure behaviour under high test rates is increasing. So far, there is no robust technique for measuring the strain energy release rate. Different testing and analysis techniques have been presented and research shows contrantive results [3-5]. In the present work, a testing methodology assessing the critical strain energy release rate at

Mode I and Mode II is presented. It includes testing under various test speeds to investigate if there is any change in the parameter Δ in Mode I configuration, the delamination correction length (in mm) that accounts for the beam not being perfectly built-in (that is, rotation may occur at the delamination front) and the shear deformation at the root of the beam [1, 6].

2. Materials, Specimens and Test Plan

The matrix was HexPly® 8552 reinforced with AS4 (12K). Specimens were laid up using the Automated Fibre Placement technique in a (0_{24}) stacking sequence. An insert film of Tygavac RF260 material 20 μm thickness was laid up in the mid-plane, through the thickness of the laminate to produce the initial delamination for the fracture tests in a nominal length of 50 mm [7]. Aluminium hinges were bonded at the end of each specimen containing the film insert to enable load application. For the Mode I test specimens two hinges were bonded, while for the Mode II only one hinge was bonded. Hinges were not bonded in the specimens used in the wedge test procedure.

In terms of test rates, they varied in the range of 0.1 mm/min to 1 m/s. In that way, the parameter Δ could be assessed for a range of test rates and provide an indication of the behaviour at the highest test speed, since, it would not be possible to be calculated [8].

3. Experimental Methods

3.1 Mode I

3.1.1 Double Cantilever Beam (DCB)

The quasi-static DCB specimen tests were performed on a screw-driven universal testing machine (Lloyds 5K) equipped with a 1 kN load cell (Fig. 1). DCB tests were conducted following ASTM D5528 [1]. The average thickness and width values were used for the calculation of Mode I interlaminar fracture toughness, G_{Ic} . One edge of each test specimen was coated with white correction fluid. In one specimen a grid marked on the side of the specimen (tested at 0.5 mm/min). Lines were marked at 1 mm intervals to a total delamination length of 100 mm. For all specimens, the hinge was clamped tightly in the test grips with the specimen aligned. Displacement was applied at a rate of 0.1, 0.5, 6 and 120 mm/min.

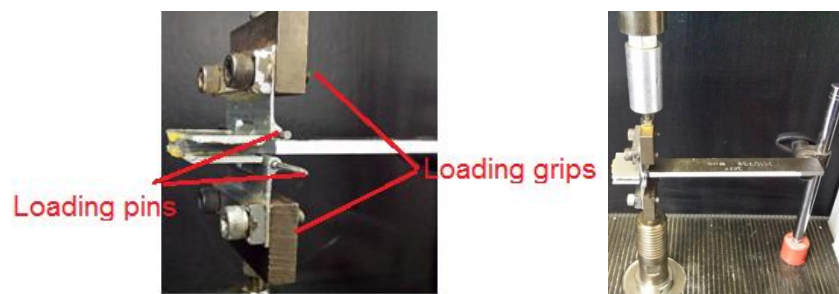


Figure 1. Mode I DCB test configuration

As the load increased the delamination length, α , was measured on one side of the test specimen using a microscope at lower test rates (up to 0.5 mm/min). Throughout the test, the load-displacement trace was recorded. At the higher test rates it was not possible to manually record the delamination growth, as a result the test was recorded using a digital camera (Sony HDR-CX700V). The camera was possible to record in high definition quality (1920x1080) with a frame rate of .30 fps.

The analysis of all the quasi-static test results was performed using the Modified Beam Theory (MBT) as described in the ASTM D5528 standard procedure [1]. All the experimental results were corrected for that machine deformation. Up to the critical point at which the compliance of the test could be assessed the parameter Δ was calculated for each test rate and any changes due to the test rate were recorded.

3.1.1 Wedge Test

In order to reach test rates up to 1m/s, it was decided to abandon the DCB test and use a wedge test configuration instead. Based on the literature, this was a more appropriate test setup to eliminate instabilities due to dynamic effects and ensure the symmetrical opening of the arms [5, 8-12]. The material of the wedge was selected to be stainless steel, which is stiff enough to minimize any deformation at the tip. Additionally, there was a radius of 1.5 mm at the tip. Furthermore, the wedge was designed to have only the 75% of the width of the specimen in order to avoid any contact close to the free edges of the specimen [12]. Prior to testing, and in order to investigate the effect of friction in measuring the G_{Ic} , a friction test took place.

At test rate of 1m/s the critical load could not be used due to noise in the loadcell. As a result, G_{Ic} was calculated according to [12], adding the correction factor Δ based on the observations of the static tests (Eq. 1). This methodology is noted as **No Load** for the needs of this study. For validation reasons No Load technique was applied to calculate G_{Ic} for DCB tests and results were compared to those from MBT.

$$G_{Ic} = 9EI\delta^2 / [4b (a + |\Delta|)^4] \quad (1)$$

In Eq.1 $I=(bh^3)/12$ with b the width and h the half thickness of the specimen. It has to be mentioned that the opening displacement of the arms, δ , was constant, unchanged and equal to the thickness of the wedge ($t=3$ mm) at the loading point during the test. Additionally, the delamination length, a , was measured from the loading point, the wedge tip, which remained immobile during the experiment. The parameter Δ was calculated from the quasi-static DCB specimens. Throughout the tests the pushing force and vertical displacement were recorded from the MTS machine [33]. Also, a high speed camera was used to video record the test and the delamination growth. This was an Olympus i-SPEED 3 with a maximum recording rate of 150,000 frames per second. The optics incorporated a 105 mm, f/2.8 lens and the system was placed on a static tripod (Fig. 2).

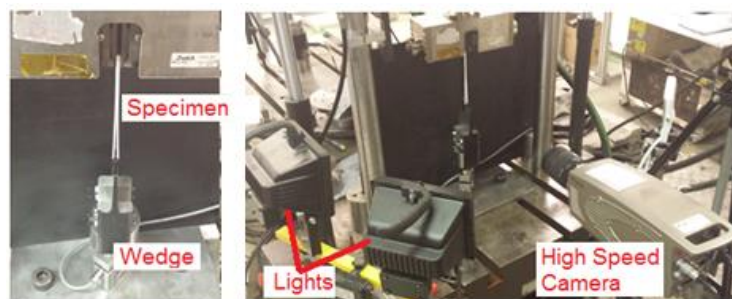


Figure 2. Wedge test configuration

3.2 Mode II

The End-Loaded Split (ELS) tests were conducted following the procedures described in ISO 15114 [2]. For all specimens, the free length, L , was set to 100 mm. All specimens were pre-cracked at

55 mm to brake any possible resin rich area ahead the foil, which could lead to an unstable delamination growth. The average values of the specimen thickness and width were used for the calculations of Mode II critical interlaminar fracture toughness, G_{IIc} . One edge of each test specimen was coated with white correction fluid and marked with lines every 1 mm, allowing the easier location of the delamination tip after delamination propagation. As the load increased the delamination length, α , was measured on one side of the test specimen using a microscope at approximately x25 magnification for the lower test rates (up to 0.5mm/min). Displacement was applied at a rate of 0.1, 0.5, 6 and 120 mm/min. The highest test rate applied was 0.18 m/s. Throughout the tests, the load-deflection trace was recorded.

The analysis of all the quasi-static test results was performed using the Standard Beam Theory (SBT) and Corrected Beam Theory using effective crack length (CBTE) as described on the ISO 15114 standard test procedure [2].

However, at the highest test rate the compliance could not be determined accurately, since oscillations were presented in the load. In that way G_{IIc} was calculated followed the static solution from Blackman [13] (Eq. 2), again noted as *No Load*. Similarly, to Mode I tests, G_{IIc} was calculated for tests performed at lower rates using No Load method and compared to CBTE values.

$$G_{IIc} = 9\delta_c^2 h^3 E_{11} (\alpha + \chi_{II} h)^2 F / [3 (\alpha + \chi_{II} h)^3 + (L + 2\chi_{II} h)^3]^2 \quad (2)$$

With $\chi_I = \Delta/h$ and $\chi_{II} = 0.42\chi_I$ obtained by Wang and Williams [14]. A photograph of the Mode II test fixture is shown in Fig. 3.

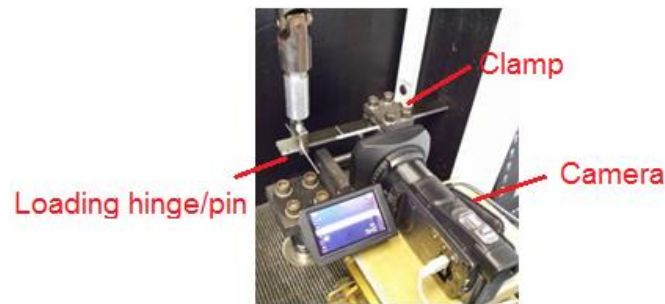


Figure 3. Mode II test configuration

3.3 Data Analysis

Image and data analysis were performed for the Mode I and II tests. Through video and image processing the delamination length was calculated and related to the corresponding load and displacement, using the time as the linkage parameter.

3.3.1 Mode I delamination length

In the case of Mode I tests, an image processing procedure was followed to crop the images around the specimen to reduce the data and load them as a matrix of binary values (0=black pixel and 1=white pixel). In that way the algorithm was capable to understand the location of the specimen (white pixels) and the background. A stepping procedure was used to find the delamination front (in pixels), which then was scaled to length (mm) by having as origin the thickness of the specimen Fig. 4.

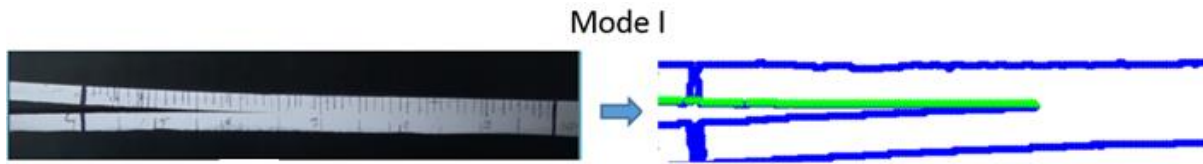


Figure 4. Extracted frame and delamination determination in Mode I

3.3.2 Mode II delamination length

In Mode II tests, since there was not a significant change in the contrast (no opening of the arms to present the difference between black and white), the software was “blind” and could not determine the delamination growth. In that way, the software required from the user to observe the different frames (images) and record the delamination length (Fig. 5).

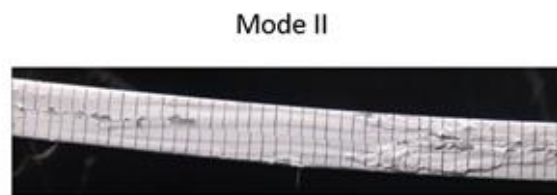


Figure 5. Extracted frame and delamination determination in Mode II

4. Experimental Results

4.1 Mode I

In Fig.6 a summary of the load - displacement curves of the tested specimens is shown. The curves have been divided into different colour categories, such as greyscale indicates test rates at 0.1 mm/min, blue 0.5 mm/min, red scale 6 mm/min and green 120 mm/min. In all graphs, load and displacement increased linearly up to the point where delamination initiated from the tip of the insert. Then, there is a gradual reduction in the load, while the displacement continued to increase and delamination propagated in a stable manner. At the final stage, the specimen was unloaded with load returning to zero.

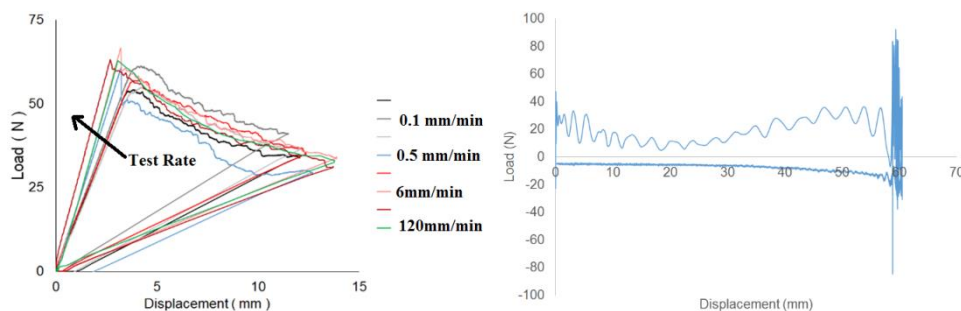


Figure 6. Load - Displacement plots of different test rates up to 120 mm/min (left) and 1 m/s (right)

Although the maximum load prior to delamination initiation did not change significantly with the test rate, however the loading slope was found higher with increasing test rate. Additionally, as the test rate

became higher, there was an unstable delamination initiation, which is indicated as an instant drop in the load from the maximum value. This is most probably caused due to the viscoelastic behaviour of the resin ahead the delamination tip. With the increase of test rate of about 5 times (0.1 to 0.5 mm/min) the process zone ahead the delamination tip (Fig. 7) became less ductile, more brittle and hence leading to an unstable delamination growth [15].

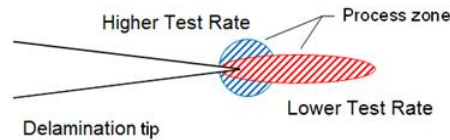


Figure 7. Schematic representation of process zone ahead of the delamination tip under mode I loading for low and high test rate conditions

Then, according to the ASTM D5528 standard for Mode I tests [8], the parameter Δ was calculated as shown in Fig. 8, by plotting the linear fit of the cube root of the compliance, $C^{1/3}$, against the measured delamination length, α . When these values were compared to data produced previously for the same material tested at 0.5 mm/min values [7] a good correlation was found as it can be seen in Fig. 8.

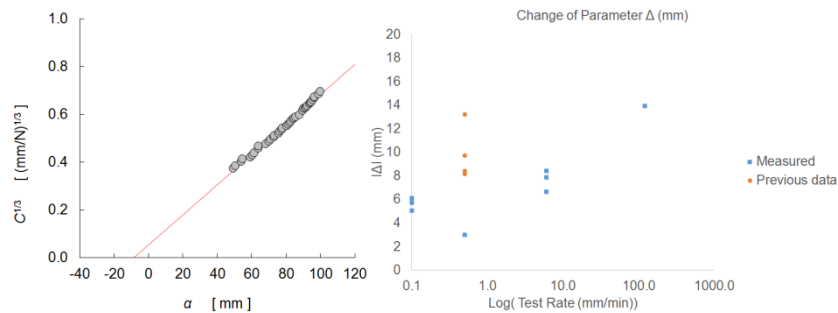


Figure 8. Determination of parameter Δ (left) and changes with different test rates (right)

The comparison with older values indicated that parameter Δ is independent to test rate and is related to the geometry properties. As a result, at higher test rates in which it was not possible to be determined due to lack of load data, an average value (from the current and older provided data) of Δ (8.03 mm) and χ_I (3.58) could be used.

At test rates higher than 120 mm/min Mode I tests were performed with the wedge configuration, in which dynamic effects are clearly noticed by the oscillations of the load (Fig. 6). However, the propagation of the delamination was in a stable manner.

4.2 Mode II

In Fig. 9 a summary of the load - displacement curves of the tested specimens is shown. The curves have been divided into different colour categories, such as greyscale indicates test rates at 0.1 mm/min, blue 0.5 mm/min, red scale 6 mm/min and green scale 120 mm/min. Graphs were presented a linear increase with the displacement up to the maximum value, followed by a significant drop in the load and then the unloading of the specimen. There is a difference for the specimens tested at 120 mm/min, since there was an increase in the load after the drop, which occurred because the delamination had reached the clamp.

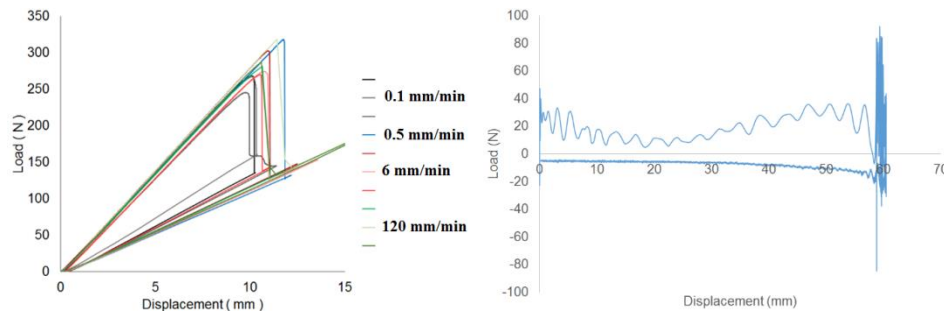


Figure 9. Load - Displacement plots of test rates up to 120 mm/min (left) and 0.18 m/s (right)

As it is evident from at Fig. 9, with increasing test rate the drop in the load was instant. The difference in the behaviour is possibly related to the process zone ahead the delamination tip. Several researchers have shown that separating the shear stress ahead of the delamination tip in the principal stress, leads to a tensile stress inclined at an angle of 45° to the laminate plane. As a result, angled cracks develop in the matrix ahead of the delamination tip, which are growing as the load increases, converge and create the S-shaped cusps [16]. With increasing test rate probably there was not enough time for the inclined cracks to merge and the delamination growth process to extend, leading to an unstable growth manner.

5 Discussion

In Mode I, the parameter Δ was found to be independent to the test rate and was related to the specimen/material properties. In addition, the G_{Ic} was calculated for the point of deviation from linearity (G_{Ic}^{NL}) and the point that 5% change of the initial compliance occurs ($G_{Ic}^{5\%}$). Delamination was propagated under a constant G level (G_{Ic}^{Prop}). Comparison graphs can be found in Fig. 10 . In all graphs, the regression lines were plotted based on the MBT values, which is the most applied method and were extended to include results for the higher rate tests. All methods presented results in the same range, however some specimens using the *No Load* methodology were found to have higher values of G_{Ic} . This was related to the displacement captured during the test, which for these specimens was higher compared to others. Moreover, it could be related to the variations in back calculated Modulus compared to the initial value that were noticed. Additionally, wedge tested specimens showed a trend for higher G_{Ic} values, however the change was not significant and the amount of tested specimens was not enough to get a safe conclusion.

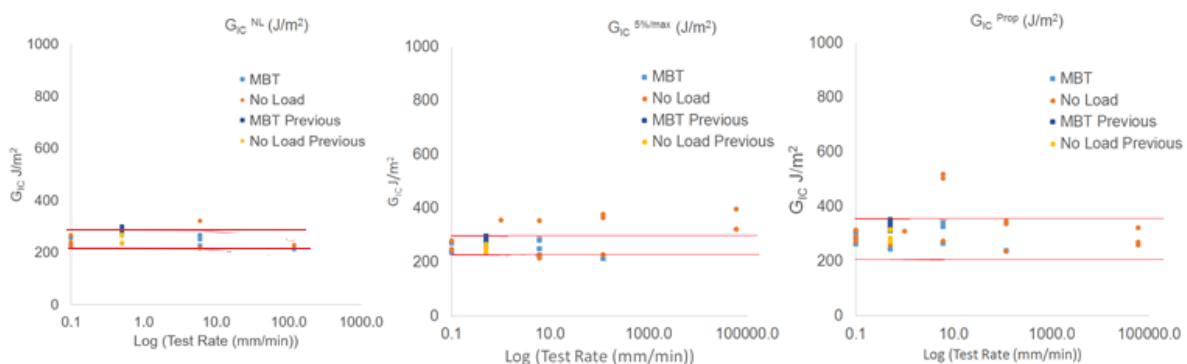


Figure 10. Comparison of G_{Ic} values for the different test rates

In Mode II, the delamination growth was unstable in all test rates, as a result no propagation values of G_{IIc} were calculated. A comparison of initiation values of G_{IIc} at the point of deviation from linearity (G_{IIc}^{NL}) and the point of maximum load occurred (G_{IIc}^{max}) are presented in Fig. 11. In both graphs, the regression lines were plotted based on the CBTE values, which is the most applied method and were extended to include results for the higher rate tests. The lowest values for G_{IIc} were found using the SBT, since it requires the measured delamination length, which does not account the effects of beam root rotation and transverse shear. No Load technique was found in between the SBT and CBTE giving confidence for calculating the G_{IIc} at higher test rates. It is shown that the changes in G_{IIc} related to test rate were insignificant, as it was found in [13].

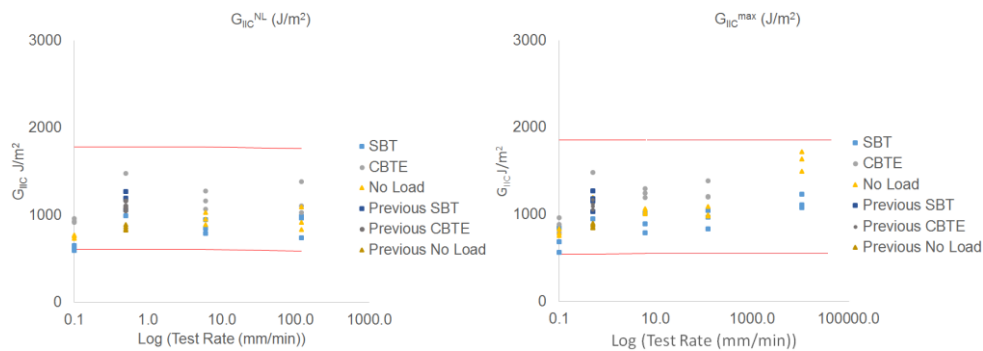


Figure 11. Comparison of G_{IIc} values for the different test rates

5 Conclusions

To summarise, the investigation of different test rates at Mode I and Mode II configurations did not present a significant effect on the fracture toughness of the material. Although a trend of increasing it was noticed at the highest test rates, the amount of tested specimens does not allow to obtain a safe conclusion. However, there were indications that different test rates affect the fracture surfaces from the load-displacement curves, in both test configurations. The wedge configuration test provided similar results to the DCB test setup, however improvements are needed for evaluating the opening force of the arms on the specimen.

Acknowledgments

The authors would like to express gratitude to Dr.-Ing. Sabine Frenz for her support and suggestions given on this project. The contributions of Dr Amirhossein Hajdai were instrumental in performing the high speed tests and very much appreciated. The assistance of Mr. Dave Sadler in completion of the low rate testing was also very important. Additionally, many thanks to Mr. Konstantinos Antoniadis and Mr. Theocharis Alexopoulos for their important contributions and suggestions in building the delamination recognition software.

References

- [1] Standard Test Method for Mode I Interlaminar Fracture Toughness of Unidirectional Fiber-Reinforced Polymer Matrix Composites, ASTM Standard D5528 -13. Philadelphia, PA: American Society for Testing and Materials; 2013.
- [2] BSI Standards Publication, Fibre-reinforced plastic composites - Determination of the mode II fracture resistance for unidirectionally reinforced materials using the calibrated end-loaded split

- (C-ELS) test and an effective crack length approach, BS ISO 15114. : The British Standards Institution; 2014.
- [3] Friedrich K, Walter R, Carlsson LA, Smiley AJ, Gillespie JW, J. Mechanisms for rate effects on interlaminar fracture toughness of carbon/epoxy and carbon/PEEK composites. *Journal of Materials Science*, 24(9): 3387-98, 1989.
 - [4] Brunner AJ, Blackman BRK, Davies P. A status report on delamination resistance testing of polymer-matrix composites. *Engineering Fracture Mechanics*, 75(9): 2779-94, 2008.
 - [5] Cantwell WJ, Blyton M. Influence of loading rate on the interlaminar fracture properties of high performance composites - A review. *Applied Mechanics Reviews*, 52(6) 199-212, 1999.
 - [6] Hodgkinson JM. *Mechanical testing of advanced fibre composites*. Woodhead Publishing Limited, 2000
 - [7] Giannis S. Novel Test Methods: Coupon Level Test Data and Analysis Quasi-static and Fatigue Delamination Characterisation of CFRP Composite Materials. Report number: C1997-2; 2009.
 - [8] Blackman BRK, Dear JP, Kinloch AJ, MacGillivray H, Wang Y, Williams JG, et al. Failure of fibre composites and adhesively bonded fibre composites under high rates of test part I mode I loading-experimental studies. *Journal of Materials Science*,30(23): 5885-5900, 1995.
 - [9] Kusaka T, Hojo M, Mai Y, Kurokawa T, Nojima T, Ochiai S. Rate dependence of mode I fracture behaviour in carbon-fibre/epoxy composite laminates. *Composites Science and Technology*, 58(3-4): 591-602, 1998.
 - [10] Joannic R, Chartier B. Device for utilizing the DCB test geometry at intermediate opening velocities. *Journal De Physique.IV : JP*, 10(9) 249-254, 2000.
 - [11] Hug G, Thevenet P, Fitoussi J, Baptiste D. Effect of the loading rate on mode I interlaminar fracture toughness of laminated composites. *Engineering Fracture Mechanics*, 73(16) 2456-2462, 2006.
 - [12] Dillard DA, Pohlit DJ, Jacob GC, Starbuck JM, Kapania RK. On the use of a driven wedge test to acquire dynamic fracture energies of bonded beam specimens. *Journal of Adhesion*, 87(4) 395-423, 2011.
 - [13] Blackman BRK, Dear JP, Kinloch AJ, MacGillivray H, Wang Y, Williams JG, et al. The failure of fibre composites and adhesively bonded fibre composites under high rates of test. III. Mixed-mode I/II and mode II loadings. *Journal of Materials Science*, 31(17): 4467-77, 1996.
 - [14] Wang Y, Williams JG. Corrections for mode II fracture toughness specimens of composites materials. *Composites Science and Technology*, 43(3): 251-256, 1992.
 - [15] Papanikolaou G. *Viscoelasticity*. University of Patras, 2007
 - [16] Greenhalgh E.S. *Failure Analysis and Fractography of Polymer Composites*. Woodhead Publishing Limited, 2009.